Journal of Materials and
Environmental Sciences
ISSN : 2028-2508
CODEN : JMESCN

J. Mater. Environ. Sci., 2018, Volume 9, Issue 1, Page 172-188

https://doi.org/10.26872/jmes.2018.9.1.21

http://www.jmaterenvironsci.com

Synthesis and characterization of new quinoxaline derivatives of 8-hydroxyquinoline as corrosion inhibitors for mild steel in 1.0 M HCl medium

M. Rbaa[1], M. Galai[2], M. El Faydy[1], Y. Lakhrissi[1],
M. EbnTouhami[2], A. Zarrouk[3], B. Lakhrissi[1*]
[1]*Laboratory Agro-Resources, Polymers and Process Engineering, Faculty of Sciences,*
Ibn Tofail University, PO Box 133, 14000, Kénitra - Morocco
[2]*Laboratory of Materials Engineering and Environment: Application and Modeling, Faculty of Sciences,*
Ibn Tofail University, PO Box 133, 14000, Kénitra - Morocco
[3]*LC2AME, Faculty of Sciences, Premier Mohammed University, PO Box 717, 60 000, Oujda - Morocco*

Received 17 Apr 2017,
Revised 26 Aug 2017,
Accepted 31 Aug 2017

Keywords

- ✓ Quinoxaline,
- ✓ Hydroxyquinoline,
- ✓ Mild steel,
- ✓ HCl,
- ✓ Corrosion,
- ✓ Inhibition,
- ✓ Electrochemical techniques,
- ✓ SEM

Pr. B. Lakhrissi
b.lakhrissi2012@gmail.com
LAKHRISSI.BRAHIM@uit.ac.ma
Tel.: **+212 6 11 17 41 49**

Abstract

Two newly substituted quinoxalines derivatives of 8-hydroxyquinoline, namely 1,4-bis-((8-hydroxyquinolin-5-yl)-methyl)-6-methylquinoxalin-2,3-(1H,4H)-dione **(Q-HNHyQ)** and 1,4-bis-((8-hydroxyquinolin-5-yl)-methyl)-quinoxalin-2,3-(1H,4H)-dione **(Q-CH_3NHyQ)**, were synthesized and characterized by ^{1}H and ^{13}C NMR spectroscopy. Their inhibitory performance was investigated against the corrosion of mild steel in 1 M hydrochloric acid medium by various corrosion monitoring techniques, such as weight loss, Tafel polarization and electrochemical impedance spectroscopy (EIS). It was found that the studied compounds exhibit a very good performance as corrosion inhibitors for mild steel corrosion in 1 M HCl. The inhibition efficiencies obtained from all employed methods are in good agreement with each other. It has been determined that the adsorption for the studied inhibitors on mild steel complies with the Langmuir adsorption isotherm at all studied temperatures. Potentiodynamic polarization studies have shown that the studied compounds act as mixed-type inhibitors toward mild steel. Scanning electron microscopy (SEM) was performed and discussed for surface study of uninhibited and inhibited mild steel samples.

1. Introduction

Steel are present with very high percentages in industrial sectors such as (technological industry, construction sectors) [1] despite a large amount of steel is destroyed by corrosion in harsh environments especially in acidic environments. Corrosion therefore affects most industries and can cost billions of dollars each year [2] at an economical level. So, stopping or at least slowing this damage became mandatory.

The broad use of acid solutions in the industries (manufacturer fertilizer industries [3], metallurgical industry, particularly for descaling, pickling of metals and cleaning of industrial plants or metals) [4], is widely characterized by the synthesis of organic and inorganic chemicals, but despite the aggressiveness of these in acidic solutions [5], the only solution to overcome this undesirable problem presenting organic inhibitors became mandatory to stop the deterioration of the metal [6]. Their selection depends on the type of acid, its concentration, the temperature and the metal material exposed to the action of the [7] acid solution.

The injection of organic inhibitors to the aggressive medium has been proven to be an effective and practical way to reduce the corrosion process on metal [8-14]. Some heterocyclic compounds were found to be good corrosion inhibitors in deferent environments. Heckerman recommended the use of sulfur-containing compounds for inhibiting corrosion in sulfuric medium and compounds containing nitrogen in the middle of hydrochloric acid [15], whereas the compounds containing heteroatoms of nitrogen showed a better inhibitory efficacy in hydrochloric acid media as long as the sulfur atoms contain compounds in inhibiting corrosion in sulfuric medium [16,17], and since most of compounds containing nitrogen and sulfur would be better than a compound containing only nitrogen, or sulfur [18].

Quinoxalines proved to be a good corrosion inhibitor of mild steel in acid media. For example 2-phenylthieno-(3,2-b)-quinoxaline, 2-[3-(2-oxo-2-phenylethylidene)-1,4-dihydroquinoxalin-2(1H)-ylidene]-1-phenylethanone, 2-ethyl-(4-(2-ethoxy-2-oxoethyl)-2-p-tolylquinoxalin-1-(4H)-yl)-acetate, Acenaphtho[1,2-b],[(3E)-3-(2-oxo-2-phenylethylidene)-3,4-dihydroquinoxalin-2-(1H)-ylidene]-1-phenylethanone, 4-(quinoxalin-2-yl)phenol , xanthone, 3,7-dimethylquinoxalin-2(1H)-one and 3,7-dimethylquinoxaline-2(1H)-thione quinoxaline showed inhibitory efficiencies mild steel corrosion in HCl medium 1 M hydrochloric acid, which is greater than 90 % [19-26].

Also, in our previous work, we showed that some 8-hydroxyquinolines derivatives are excellent inhibitors for carbon steel in acidic solutions [27,28]. This encourages us to synthesize more compounds of this family and to test them as corrosion inhibitors in acidic medium. In this contribution, two new compounds based on 8-hydroxyquinoline namely 1,4-bis-((8-hydroxyquinolin-5-yl)-methyl)-6-methylquinoxalin-2,3-(1H,4H)-dione (**Q-HNHyQ)** and 1,4-bis-((8-hydroxyquinolin-5-yl)-methyl)-quinoxalin-2,3-(1H,4H)-dione (**Q-CH$_3$NHyQ)** have been successfully synthesized and tested for the inhibition action on the corrosion of mild steel in 1 M HCl, using weight loss and polarization techniques. The structures of these compounds are confirmed by ^{1}H and ^{13}C NMR spectroscopy.

2. Experimental section

2.1. Description of materials and products

All used chemicals in this study are from Aldrich or Acros Spain or France. Melting points were determined on an automatic electrothermal IA 9200 digital melting point apparatus in capillary tubes and are uncorrected. The recording of NMR spectra was performed on a Bruker Advanced 300 WB at 300 MHz for solutions in Me$_2$SO-d$_6$ and chemical shifts are given in δ_{ppm} with reference to tetramethylsilane (TMS) as an internal standard. The progress of the reaction is followed by chromatography with thin layer (TLC) of silica 60 F254 (E. Merck).

The mild steel samples were used with 0.09 % P, 0.38 % Si, 0.01 % Al, 0.05 % Mn, 0.21 % C, 0.05 % S and the remainder of iron. Before any measurement, they were abraded with a series of emery paper grades 180-1200. The specimens are thoroughly washed with double distilled water, degreased with acetone and then dried. The aggressive solution 1 M HCl was prepared by the dilution of concentrated HCl (37 %) analytical grade with bi-distilled water.

2.2. Chemical synthesis and characterization

*2.2.1. Synthesis of quinoxaline-2,3-diones (**QH**) and 6-methylquinoxaline-2,3-diones (**QCH$_3$**)*

The synthesis of **QH** and **QCH$_3$** was carried out by the condensation of the corresponding *o*-phenylenediamine with the hydrated oxalic acid according to the method described by Ohmori et al. [29] (scheme 1):

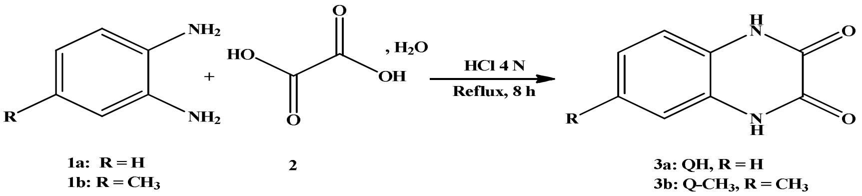

Scheme 1: Synthetic route for the preparation of **QH** and **QCH$_3$**

*2.2.2. Synthesis of 5-chloromethyl-8-hydroxyquinoline hydrochloride (**CMHQH**)*

The preparation of 5-chloromethyl-8-hydroxyquinoline hydrochloride (**CMHQH**) was realized according to the method described by Fen et al. [30], which consists of the reaction of 8-hydroxyquinoline (**HyQ**) with formaldehyde 40 % and concentrated HCl solution 37 % , the reaction mixture was treated with dry gaseous hydrogen chloride for 24 hours (scheme 2).

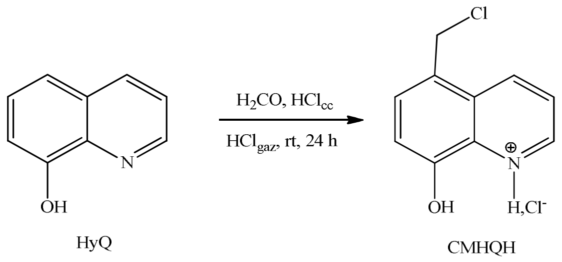

Scheme 2: Synthesis of 5-chloromethyl-8-hydroxyquinoline hydrochloride **CMHQH**

2.2.3. General procedure for the synthesis of ***Q-HNHyQ*** and ***Q-CH$_3$NHyQ***

The synthesis of 1,4-bis-((8-hydroxyquinolin-5-yl)-methyl)-quinoxaline-2,3-(1H,4H)-dione (**Q-HNHyQ)** and 1,4-bis-((8-hydroxyquinolin-5-yl)-methyl)-6-methylquinoxaline-2,3-(1H,4H)-dione (**Q-CH$_3$NHyQ)** is done by the following scheme 3.

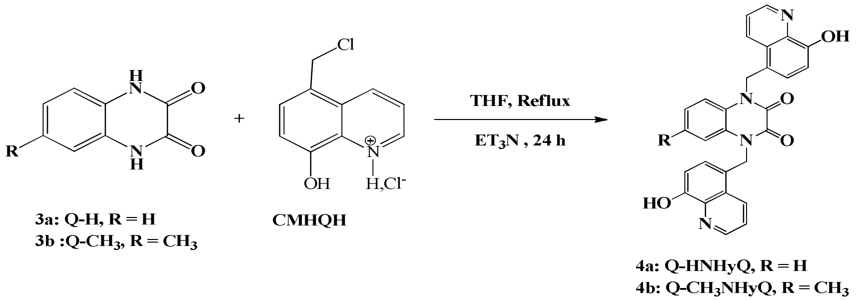

Scheme 3: Synthetic route for the preparation of **Q-HNHyQ** and **Q-CH$_3$NHyQ**

A mixture of quinoxaline (0.01 mole) and 5-chloromethyl-8-hydroxyquinoline hydrochloride (0.002 mole) in 50 ml of tetrahydrofuran in the presence of (0.03 mole) of triethylamine was refluxed with magnetic stirring for 24 h. The progress of the reaction was monitored by TLC until completion. After evaporation of the solvent under reduced pressure, the obtained residue was hydrolyzed, extracted with chloroform (3 x 20 ml). The combined organic phases were washed twice with saturated aqueous sodium chloride, dried over anhydrous MgSO$_4$ and evaporated in vacuo to give the crude product, which was recrystallized from EtOH. The structure, product name and abbreviation were given in Table 1.

2.2.3.1. Synthesis of 1, 4-bis ((8-hydroxyquinolin-5-yl)-methyl)-quinoxaline-2,3(1H,4H)-dione (***Q-HNHyQ***)

It was synthesized from quinoxaline-2,3-(1H,4H)-dione and 5-chloromethyl-8-hydroxyquinoline hydrochloride ride following the general procedure. Yield 75 %, yellow solid, mp > 260 °C, R$_f$ value: 0.43 (hexane/acetone: 4/6).

^{1}H RMN (Me$_2$SO-d$_6$, 300 MHz), δ = 4.85 (S, 2H, OH), 5.37 (S, 2H, CH$_2$), 7.48-8.77 (m, 4H, aromatic of quinoxaline), 7.10-7.45-7.45-8.48-8.77 (m, 10 H, aromatic of quinoline).

^{13}C RMN (Me$_2$SO-d$_6$, 300 MHz): δ = 46.08 (CH$_2$), 150.67 (ArC-OH), 153.86 (C=O) 127.03-122.95 (ArCH benzene of quinoxaline), 131.18 (ArCH benzene of quinoxaline), 112.87-121.24-127.80-131.18-148.27 (ArCH of quinoline).

2.2.3.2. Synthesis of 1,4-bis-((8-hydroxyquinoline-5-yl)-alkyl)-6-methylquinoxaline-2,3-(1H,4H)-dione (***Q-CH$_3$NHyQ***)

It was synthesized from 6-methylquinoxaline-2,3-(1H,4H)-dione and 5-chloromethyl-8-hydroxyquinoline hydrochloride following the general procedure. Yield 80 %, brown solid, mp > 260 °C, R$_f$ value: 0.38 (hexane/acetone: 4/6).

^{1}H RMN (Me$_2$SO-d$_6$, 300 MHz): δ = 2.37 (S, 3 H, CH$_3$), 5.33 (S, 2H, OH), 3.91 (S, 2 H, CH$_2$), 7.04-7.04-7.06-7.41-7.46 (m, 10 H, aromatic of quinoline), 6.54-7.09-7.25 (m, 3 H, aromatic of quinoxaline).

^{13}C RMN (Me$_2$SO-d$_6$, 300 MHz): δ = 46.12 (CH$_2$), 21.57 (CH$_3$), 151.01 (ArC-OH), 152.86 (C=O) 121.77-111.23-130.30 (ArCH benzene of quinoxaline), 128.35-133.93 (ArCH benzene of quinoxaline), 110.74-122.77-126.91-128.76-148.09 (ArCH of quinoline).

Table 1. Names, chemical structures and abbreviations of the synthesized compounds

Structure	Name	Abbreviation
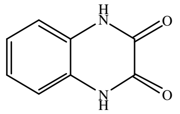	Quinoxaline-2,3-(1H,4H)-dione	**QH**
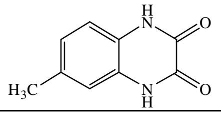	6-Methylquinoxaline-2,3-(1H,4H)-dione	**QCH_3**
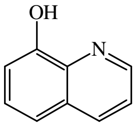	8-Hydroxyquinoline	**HyQ**
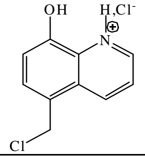	5-Chloromethyl-8-hydroxyquinoline hydrochloride	**CMHQH**
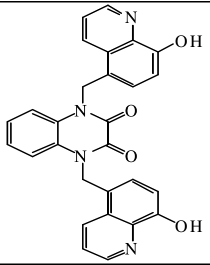	1,4-Bis-((8-hydroxyquinolin-5-yl)-methyl)-quinoxaline-2,3-(1H,4H)-dione	**Q-HNHyQ**
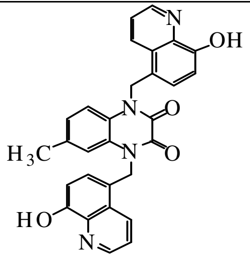	1,4-Bis-((8-hydroxyquinolin-5-yl)-methyl)-6-methylquinoxaline-2,3-(1H,4H)-dione	**Q-CH_3NHyQ**

2.3. Corrosion Inhibition Study

2.3.1. Weight loss measurements

This relatively simple method of operation is preferred to other methods that require the use of sophisticated instruments [30], but does not allow the approach of the mechanisms involved in the corrosion. It is to measure the weight loss **m** of the surface samples **S** immersed in a corrosive solution during time **t**.

The samples of defined size undergo dry manual mechanical polishing with a succession of abrasive paper of increasing particle size (120, 180, 400, 600 and 1200) then they are rinsed with double distilled water, degreased in ethanol and dried in the air. The samples were then weighed and immersed in solution so that the entire material is in contact with the solution. At the end of the corrosion, products are removed by pickling in an acid mixture and the samples were weighed again. The immersion time was fixed according to the results of our previous work [1,2,27]. The corrosion rate was determined after 6 hours of immersion at constant temperature equal to 298 K and it was calculated by the following equation (1):

$$\omega_{corr} = \frac{m_i - m_f}{S \times t} \quad (1)$$

Where mi, mf, S and t denote initial weight, final weight, surface of specimen and immersion time, respectively. The value of the inhibiting efficiency was calculated by the following equation (2):

$$\eta_{\omega}(\%) = \frac{\omega^{0}_{corr} - \omega_{corr}}{\omega^{0}_{corr}} \times 100 \quad (2)$$

Where ω^{0}_{corr} and ω_{corr} are the corrosion rates in the absence and presence of inhibitors, respectively.

2.3.2. Potentiodynamic polarization

For the electrochemical measurements, we used the potentiodynamic technique. The cell used was made of three electrodes in classic Pyrex glass with a platinum counter-electrode foil and a standard calomel electrode (SCE) as a reference. The working electrode was mild steel electrode, which has been cut from mild steel sheets having a thickness of 0.1 centimeter. The electrode dimensions were 1 × 1 cm and it was welded on one side to a copper wire used for the electrical connection, the potential intensity curves are obtained according to the potentiodynamic techniques with a scan rate of 0.5 mV/s. This speed allowed us to place ourselves in quasi-stationary conditions and to have a good reproducibility. Before the curve plot, the working electrode was biased at - 800 mV for 15 min to the stripping then maintained at the floating potential for 60 min [31].

From the obtained polarization curves, the corrosion currents (i_{corr}) were calculated by adjusting the curve using the equation (3):

$$i = i_{\mathrm{a}} + i_{\mathrm{c}} = i_{\mathrm{corr}} \left\{ \exp\left[b_{\mathrm{a}} \times \left(E - E_{\mathrm{corr}} \right) \right] - \exp\left[b_{\mathrm{c}} \times \left(E - E_{\mathrm{corr}} \right) \right] \right\} \quad (3)$$

Where β_a and β_c are the anodic and cathodic slopes of Tafel's right and ΔE difference potential

2.3.3. Electrochemical impedance spectroscopy

The impedance measurements were performed by using a VoltaLab 40, provided with a Potentiostat PGZ 100 controlled by a computer and the master Volta 4 software adapted to the impedance measurements and the potential drop in a domain frequency of 100 KHz-10 MHz. The measurement was performed in a potential range of ± 10 mV centered at the floating potential.

The effectiveness of the inhibition of the inhibitor was calculated from the transfer of the resistance values of the load by using the following equation (4).

$$\eta_{EIS}(\%) = \left(\frac{R^{i}_{ct} - R^{\circ}_{ct}}{R^{i}_{ct}} \right) \times 100 \quad (4)$$

Where R°_{ct} and R^{i}_{ct} are the charge transfer resistance in the absence and presence of an inhibitor, respectively.

3. Results and Discussion

3.1. Gravimetric Study:

The mass loss measures are the first approach to the study of the corrosion inhibition of a metal in an electrolyte solution that has the advantage of being a simple implementation and does not require significant equipment. The corrosion rate is determined after 6 hours of immersion at the temperature of 298 K to various concentrations of the two tested inhibitors. The value of this speed is given by the following relationship (1, 2). The results obtained from the gravimetric studies are summarized in Table 2. Analysis of the results in Table 2 showed clearly that **Q-CH_3NHyQ** and **Q-HNHyQ** compounds possess good corrosion inhibiting properties of mild steel in 1 M HCl medium. We also find that the corrosion rate decreases while the effectiveness of protection increases with the concentration of inhibitor and reaches a maximum value of **94.6 %** and **90.9 %** at 10^{-3} M of **Q-CH_3NHyQ** and **Q-HNHyQ** respectively.

3.2. Electrochemical impedance measurements

The electrochemical impedance spectroscopy diagrams are presented in Nyquist (Figures 1 and 2) in this study; these diagrams were recorded in the presence and absence of the organic inhibitors **Q-CH_3NHyQ** and **Q-HNHyQ**. In this case, the capacitive loop can be attributed to a charge transfer [32]. Thus, we have been able to access the values of the charge transfer resistance (R_t) and the capacity of the double layer (C_{dl}) and consequently the corrosion inhibiting efficiency of mild steel in 1 M hydrochloric medium.

Table 2. Corrosion parameters for mild steel in 1 M HCl, in the absence and presence of different concentrations of various inhibitors, from weight loss measurements at 298 K for 6 h

Inhibitor	[C] (M)	ω_{corr} (mg cm^{-2} h^{-1})	η_{ω} (%)
Q-HNHyQ	0	33.40	—
	10^{-6}	8.02	76.0
	10^{-5}	6.00	82.0
	10^{-4}	5.35	84.0
	10^{-3}	3.02	**90.9**
Q-CH$_3$NHyQ	0	33.40	—
	10^{-6}	6.22	81.4
	10^{-5}	5.15	84.6
	10^{-4}	3.88	88.4
	10^{-3}	1.79	**94.6**

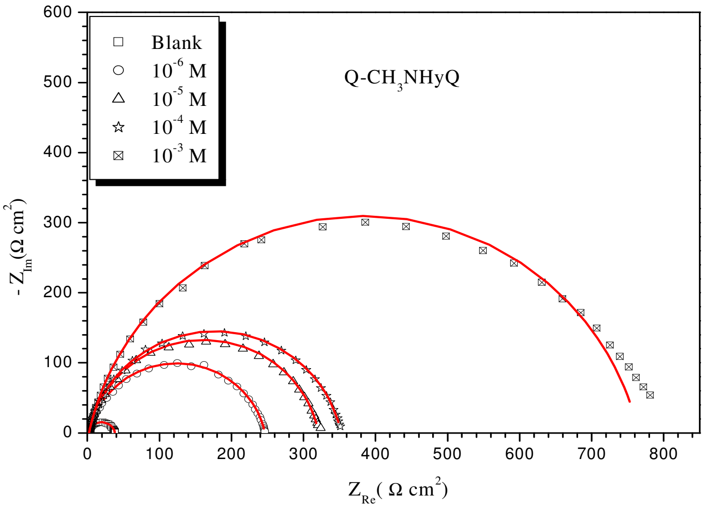

Figure 1: Nyquist plots for mild steel in 1 M HCl. At different concentrations of **Q-CH$_3$NHyQ** at 298 K

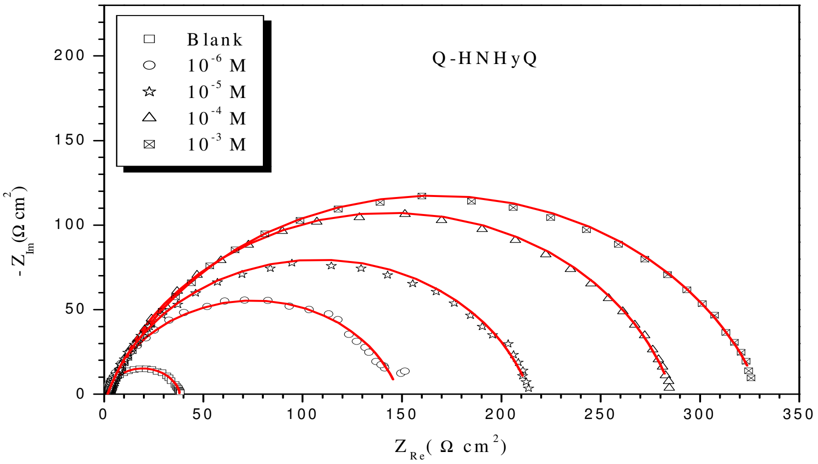

Figure 2: Nyquist plots for mild steel in 1 M HCl. at different concentrations of **Q-HNHyQ** at 298 K

From the form of diagrams presented in the Nyquist plane, the model of the equivalent circuit explaining these experimental results is given in the (Figure 3).

The impedance diagrams presented in the Nyquist plan are in the form of semicircles whose sizes increase with the inhibitor concentration, indicating a well-defined charge transfer process and improved protection in the presence of the studied organic inhibitors. However, it allowed employing CPE element in order to investigate the inhibitive film properties on metallic surface. Thus, the impedance of the CPE can be described by the following equation (5).

$$Z_{\mathrm{CPE}} = \left[Q(j\omega)^n \right]^{-1} \quad (5)$$

Where *j* is the imaginary number, *Q* is the frequency independent real constant, $\omega = 2\pi f$ is the angular frequency (rad s^{-1}), f is the frequency of the applied signal, n is the CPE exponent for whole number of $n = 1, 0, -1$, CPE is reduced to the classical lump element-capacitor (*C*), resistance (*R*) and inductance (L) [33]. The use of these parameters, similar to the constant phase element (CPE), allowed the depressed feature of Nyquist plot to be reproduced readily.

In addition, the effective calculated double layer capacitance (C_{dl}) derived from the CPE parameters according [34] to the following equation (6):

$$C_{dl} = Q^{\frac{1}{n}} \times R^{\frac{(1-n)}{n}} \quad (6)$$

The expression of the inhibitory efficiency versus load transfer resistance is given by the following equation (4).

Table 3 shows the different parameters from the electrochemical impedance measurements for the studied compounds.

The Bode plot of both experimental and simulated data of mild steel in 1.0 M HCl solution without and with 10^{-3} M of **Q-CH_3NHyQ** are shown in Figure 4.

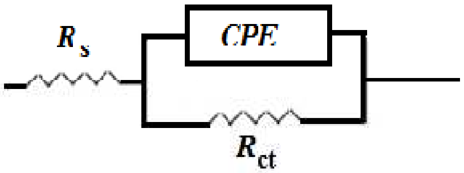

Figure 3: Equivalent electrical circuit for the interface mild steel/1 M HCl

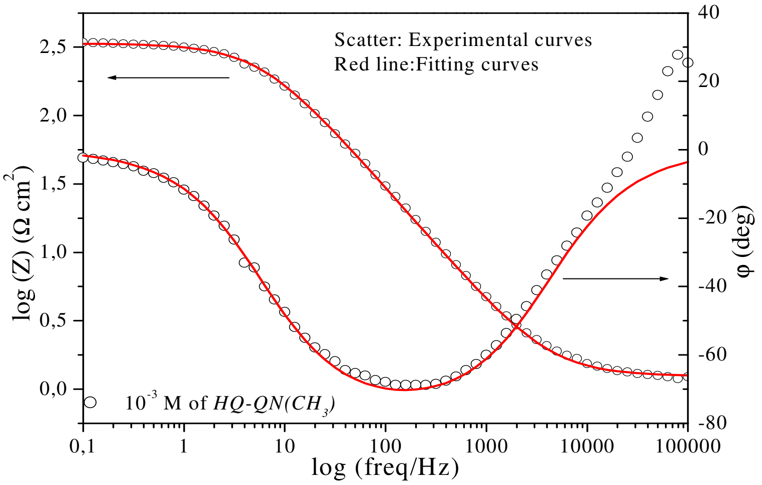

Figure 4: Bode and phase angle plots of impendence spectra for mild steel in 1 M HCl in absence and presence of optimum concentration of **Q-CH_3NHyQ** at 298 K

Table 3. Electrochemical impedance parameters for mild steel in 1 M HCl solution in the absence and presence of inhibitors concentrations of **Q-CH_3NHyQ** and **Q-HNHyQ** at 298 K

Medium	[C] (M)	R_s (Ω cm^2)	R_{ct} (Ω cm^2)	C_{dl} (μF cm^{-2})	n	η_{EIS} (%)
HCl	00	2.08	35.00	298.0	0.78	—
Q-CH_3NHyQ	10^{-3}	2.82	762.0	83.79	0.86	95.4
	10^{-4}	1.91	349.9	100.0	0.88	90.0
	10^{-5}	1.80	317.0	133.0	0.88	88.9
	10^{-6}	1.60	244.0	155.0	0.86	85.6
Q-HNHyQ	10^{-3}	2.38	328.2	93.83	0.80	89.4
	10^{-4}	2.62	283.5	128.0	0.82	87.6
	10^{-5}	1.84	212.7	132.0	0.82	83.5
	10^{-6}	1.10	148.5	215.0	0.81	76.4

In the light of the obtained results, we can make the following remarks:

These impedance diagrams are semi-perfect circles, which are associated with the dispersal of frequency due to the roughness and inhomogeneity of the surface of the electrode [35]. The electrochemical parameters such as R_{ct}, C_{dl}, and η_{EIS} (%) are located in Table 3 in which it is clear that the capacitance of the double layer C_{dl} is decreased with the addition of **Q-CH_3NHyQ** and **Q-HNHyQ** inhibitors. This reduction is associated with the adsorption of the organic molecules on the surface of the steel [36], suggesting that both **Q-CH_3NHyQ** and **Q-HNHyQ** inhibitors act by adsorption to the mild steel/solution interface [37, 38]. This situation is the result of an increase in the surface coverage by these inhibitors, which leads to an increase in the efficiency of inhibition while the R_{ct} values become larger with increasing inhibitor **Q-CH_3NHyQ** and **Q-HNHyQ**. The inhibitory efficacy of these inhibitors (η_{EIS} %) evolves in the same way as R_{ct} and reaches a value of **95.4 %** in the case of **Q-CH_3NHyQ**. But on the other hand, the **Q-HNHyQ** inhibitor is less effective than **Q-CH_3NHyQ** in 1 M HCl.

Which can be explained by the presence of the methyl group on the aromatic nucleus, which exhibits an inductive electron-donating effect (+I) in the **Q-CH_3NHyQ** inhibitor (Figure 5).

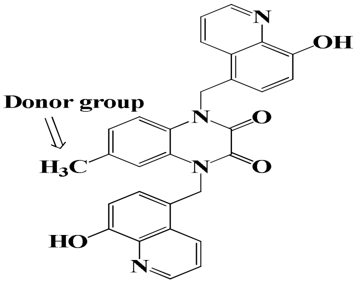

Figure 5: Inductive electron-donating effect of the methyl group

3.3. Potentiodynamic polarization

3.3.1. Effect of concentration

The Figures 6 and 7 show the curves of anodic and cathodic potential-intensities polarization of the steel in 1 M HCl medium at 298 K. In the presence and absence of inhibitor **Q-CH_3NHyQ** and **Q-HNHyQ**, and to a concentration range of 10^{-3} to 10^{-6} M, the curves have been recorded after a holding time of the working electrode to the free corrosion potential for 30 minutes. Different electrochemical parameters including corrosion potential (E_{corr}), cathodic Tafel slopes (β_c) and corrosion current density (i_{corr}) were obtained by extrapolating the polarization curve. Inhibition efficiency (η_{Tafel} %) can be calculated using Equation (7). All these parameters are listed in Table 4:

$$\eta_{Tafel}\left(\%\right) = \left(1 - \frac{i_{corr(i)}}{i_{corr}}\right) \times 100 \quad (7)$$

Where i_{corr} and $i_{corr\ (i)}$ are the uninhibited and inhibited corrosion current densities, respectively.

It is observed that the intensity-potential curves Figures 6 and 7 are moved to the positive direction to the control so maybe they are considered anodic inhibitors.

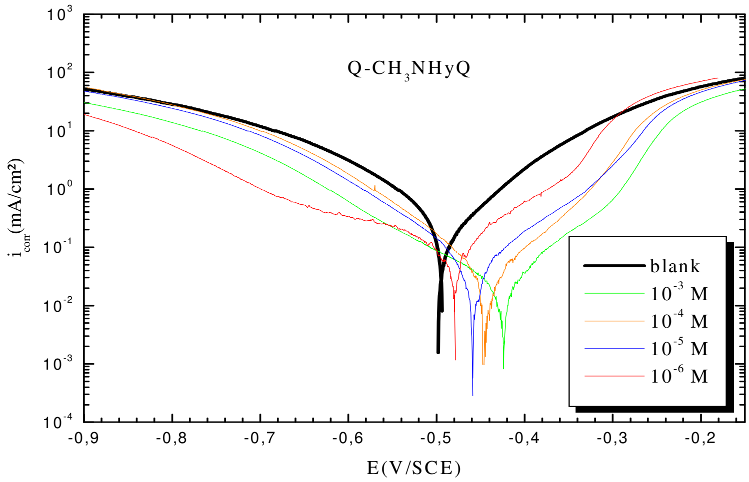

Figure 6: Tafel curves for mild steel in 1 M HCl at different concentrations of **Q-CH$_3$NHyQ** at 298 K

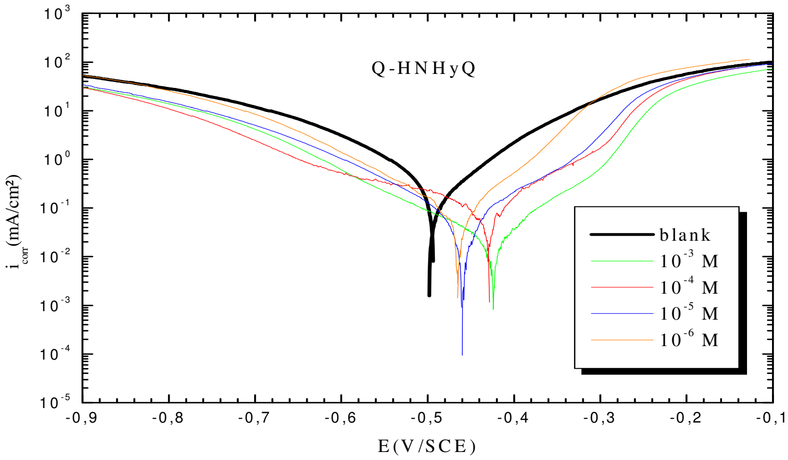

Figure 7: Tafel curves for mild steel in 1 M HCl at different concentrations of **Q-HNHyQ** at 298 K

Table 4. Electrochemical parameters **Q-CH$_3$NHyQ** and **Q-HNHyQ**

Medium	[C] (M)	$-E_{corr}$ (mV/SCE)	$-\beta_c$ (mVdec^{-1})	i_{corr} (µAcm^{-2})	η_{Tafel} (%)	θ
HCl	00	498.0	220.0	455.5	—	—
Q-CH$_3$NHyQ	10^{-6}	463.2	158.5	78.1	82.8	0.828
	10^{-5}	457.4	88.70	46.9	89.7	0.897
	10^{-4}	429.0	83.20	37.6	91.7	0.917
	10^{-3}	420.3	118.7	19.5	95.7	0.957
Q-HNHyQ	10^{-6}	478.0	96.80	122.0	73.2	0.732
	10^{-5}	458.9	101.7	84.0	81.6	0.816
	10^{-4}	446.0	114.7	68.4	84.0	0.840
	10^{-3}	424.0	123.4	48.9	89.3	0.893

The results from Table 4 indicate that the corrosion current (i_{corr}) decreases with increasing concentrations of the **Q-CH$_3$NHyQ** and **Q-HNHyQ** inhibitors, implying an inhibitory efficiency increase of these studied inhibitors, which reached a maximum value of 95 **%** for **Q-CH$_3$NHyQ**. We notice that the corrosion current density is lower in the presence of **Q-CH$_3$NHyQ** to 10^{-3} M and becomes only 19.50 µA cm^{-2}, this result means that the inhibitor **Q-CH$_3$NHyQ** is more effective than **Q-HNHyQ**, on the other hand, the addition of the tested organic products **Q-CH$_3$NHyQ** and **Q-HNHyQ** did not significantly affect the value of cathodic Tafel slope (β_c). This result indicates that the proton reduction mechanism (the slowest step) is not affected by the addition of these organic compounds [39], so the mechanism of inhibition involves a simple reaction that blocks the active sites without modifying the corrosion mechanism [40].

The decrease in the anodic and cathodic Tafel slopes indicates that inhibitors are going to retard the anodic dissolution and hydrogen evolution reactions i.e. quinoxaline derivatives are acting as a mixed type inhibitor by affecting both anodic and cathodic reactions. But the observation of E_{corr} values in presence of both compounds reveals that there is a slight shift towards positive values (Table 4) i.e. cathodic site as compared to that in their absence. Thus, the above discussion shows that the studied inhibitors are mixed-type inhibitors but predominantly anodic. The mild steel corrosion inhibition in the hydrochloric acid medium 1 M HCl can be explained in terms of adsorption on the metal surface. This process is facilitated by the presence of low-energy orbital vacancy in the iron atom. The inhibition efficiencies, calculated from Tafel impedance results, showed the same trend as those obtained from EIS, polarization and weight loss measurements (Table 5).

Table 5. Inhibition efficiency values obtained from weight loss, Tafel polarization and impedance measurements of mild steel in 1 M HCl at different concentrations of inhibitors at 298 K

Inhibitor	Inhibition efficiency η (%)			
	[C] (M)	Weight loss	Tafel polarization	Impedance
Q-CH$_3$NHyQ	10^{-6}	81.4	82.8	85.6
	10^{-5}	84.6	89.7	88.9
	10^{-4}	88.4	91.7	89.9
	10^{-3}	94.6	95.7	95.4
Q-HNHyQ	10^{-6}	76.0	73.2	76.4
	10^{-5}	82.0	81.6	83.5
	10^{-4}	84.0	84.0	87.6
	10^{-3}	90.9	89.3	89.4

3.3.2. Effect of temperature

The effect of temperature on mild steel gave us in general some information on the adsorption [41-46]. For this reason, we studied the change of the corrosion rate with the temperature in 1 M HCl solution during 1 h of immersion; both in the absence and presence of **Q-CH$_3$NHyQ** and **Q-HNHyQ** in the temperature range from 298 to 328 K, the obtained results are shown in the Figures 8-10. The electrochemical parameters are given in Table 6.

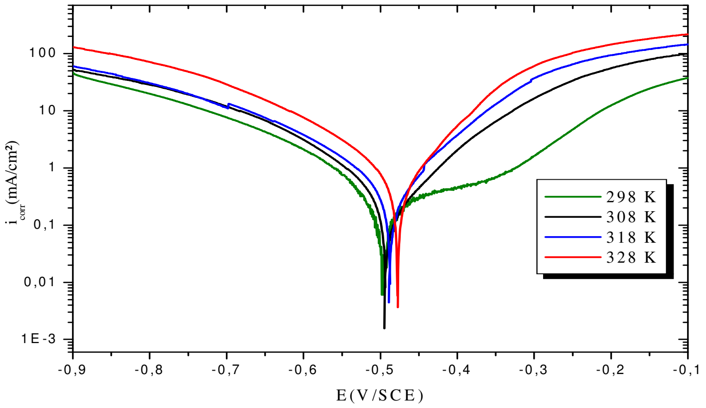

Figure 8: Polarization curves at different temperatures for mild steel in 1 M HCl without inhibitor.

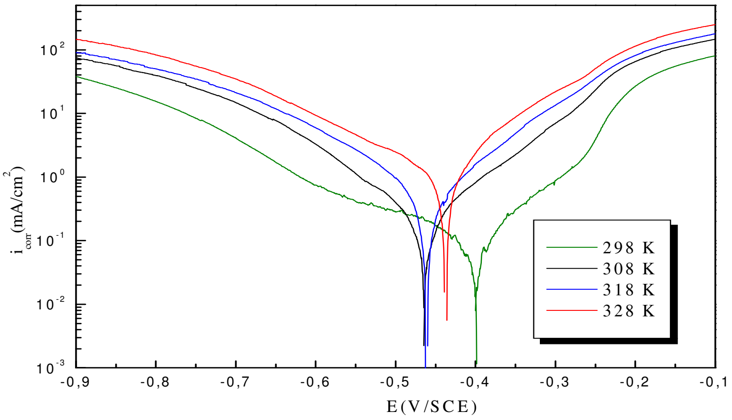

Figure 9: Polarization curves at different temperatures for mild steel in 1 M HCl in the presence of **Q-HNHyQ**

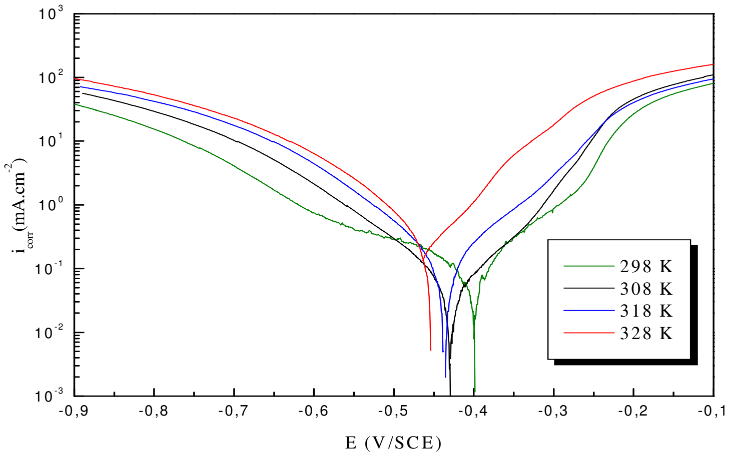

Figure 10: Polarization curves at different temperatures for mild steel in HCl in the presence of **Q-CH$_3$NHyQ**

Table 6. Evolution of the electrochemical parameters of mild steel in 1 M HCl according to temperature in the presence and the absence of inhibitors

Medium	T (K)	$-E_{corr}$ (mV SCE)	$-\beta_c$ (mV dec^{-1})	i_{corr} (μAcm^{-2})	η_{Tafel} (%)
Blank	298	459.4	220.0	467.0	—
	308	488.1	223.8	800.0	—
	318	480.2	243.3	1200	—
	328	462.4	249.3	1680	—
Q-CH$_3$NHyQ	298	420.3	118.7	19.50	**95.7**
	308	437.8	98.60	55.60	93.0
	318	443.0	91.30	120.0	90.0
	328	455.9	87.90	230.0	86.3
Q-HNHyQ	298	424.0	123.4	48.90	**89.4**
	308	462.5	106.7	180.0	77.5
	318	437.4	149.5	410.0	66.0
	328	460.8	105.8	600.0	64.3

Inspection of these results (Table 6) reveals that that the inhibitory efficiency decreases with the increase of the temperature. Also, the decrease of the inhibitory efficacy in the presence of the tested organic compounds shows that at high temperatures, these inhibitors do not exhibit a well marked adsorption on the metal surface while exhibiting a less corrosion inhibition of mild steel 1 M hydrochloric acid solution, thus applying a high temperature of these compounds is not profitable.

3.4. Kinetic parameters of activation

The activation parameters (Table 7) such as the energy of activation (E_a), the enthalpy of activation (ΔH_a), and the entropy of activation (ΔS_a) were evaluated according to the Arrhenius law [47-50] and the alternative form of the Arrhenius equation (8, 9):

$$i_{corr} = A\exp\left(\frac{-E_a}{RT}\right) \qquad (8)$$

$$i_{corr} = \frac{RT}{Nh}\exp\left(\frac{\Delta S_a}{R}\right)\exp\left(\frac{-\Delta H_a}{RT}\right) \qquad (9)$$

Where i_{corr} is the corrosion current density, R is the ideal gas constant, T is the absolute temperature, h is the Planck constant and N is the Avogadro number.

Figure 11 shows the variations of Ln i_{corr} = f (1/T) of the logarithm of the corrosion current density according to the inverse of temperature (1/T). They are used to calculate the activation energy values from the slope of each of the obtained lines. **Figure 12** shows the changes of Ln (i_{corr}/T) versus 1/T in the form of straight line with a slope of ($-\Delta H_a$/R) and the extrapolation of these lines gives the values of (Ln(R/Nh) + ΔS_a/R), hence those of ΔH_a and ΔS_a.

Inspection of Table 7 shows that apparent activation energy increases on addition of inhibitors in comparison to the blank solution. This can be explained that the studied molecules create a barrier to charge and mass transfer. The higher values of E_a in inhibited solution may also be correlated with the increased thickness of double layer, which enhances the E_a values of the corrosion reaction [51, 52]. Also the positive values of the enthalpy of activation show that the steel corrosion process is endothermic and the dissolution of steel is difficult [51]. As regards the entropy, it is used to describe the phenomenon of ordering and disordering of system, the value of ΔS_a in the absence of inhibitor is negative and tends to increase in presence of both inhibitors (Table 7). This reveals that an increase in disorder at the time when the reactants are transformed to activated complexes. Also, this may be connected to the adsorption of organic molecules was accompanied by desorption of water molecules from the metal surface [53].

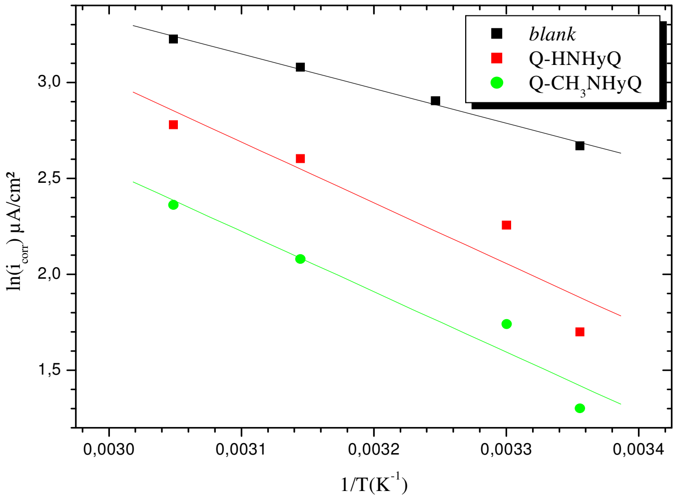

Figure 11: Arrhenius plots of mild steel in 1 M HCl in absence and presence of optimum concentration of both inhibitors.

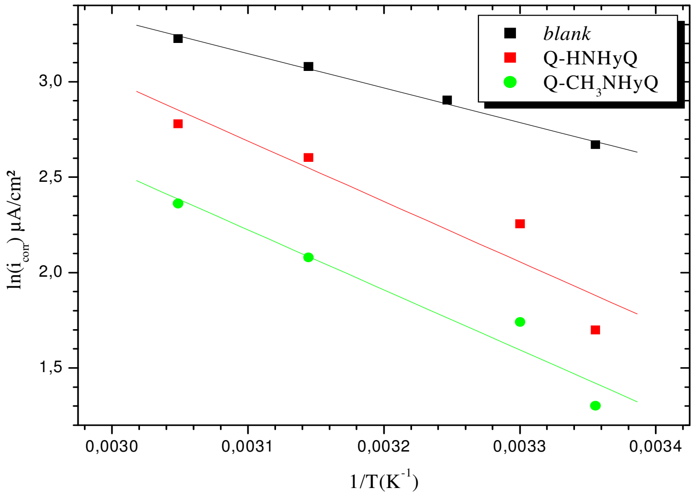

Table 12: Transition state plot for mild steel corrosion in 1 M HCl in the absence and presence of **Q-CH$_3$NHyQ** and **Q-HNHyQ** at 10^{-3} M

Table 7. Kinetics parameters of Arrhenius equation and transition state equation

Medium	E_a (kJ mol^{-1})	ΔH_a (kJ mol^{-1})	ΔS_a (J mol^{-1}K^{-1})
Blank	21.00	18.50	-126
Q-CH$_3$NHyQ	66.57	63.98	-4.57
Q-HNHyQ	68.24	65.65	-9.40

3.5. Isotherm and thermodynamic parameters of adsorption

The adsorption isotherm that describes the adsorption behavior of organic inhibitors is to know the corrosion inhibition mechanism between the inhibitor's molecules and the metal surface. Several adsorption isotherms were examined to adjust the values of the degree of the cover surface, following the Langmuir isotherm, [54-58] given by the following relationships (10):

$$\frac{C_{inh}}{\theta} = \frac{1}{K_{ads}} + C_{inh} \qquad (10)$$

Where C_{inh} is the inhibitor concentration, K_{ads} is the equilibrium constant for the adsorption-desorption process and θ is surface coverage. Surface coverage values for both inhibitors as determined by the Potentiodynamic polarization for various concentrations of the inhibitors are reported in Table 4.

Figure 13 shows the plots of C_{inh}/θ versus $_{\text{Cinh}}$ and the estimated linear correlation is obtained for the studied compounds. The strong correlation ($R^2 > 0.9999$) suggests that the adsorption of inhibitor on the mild steel surface obeyed this isotherm. Langmuir adsorption isotherm assumes that the adsorbed species occupy only one surface site and there are no interactions with other adsorbed species.

K_{ads} can be calculated from the intercepts of the straight lines, and it is correlated with the standard free energy of adsorption (ΔG^*_{ads}) by the following equation:

$$K_{ads} = \frac{1}{55.5}\exp\left(\frac{-\Delta G^*_{ads}}{RT}\right) \qquad (11)$$

Where R is the gas constant and T is the absolute temperature. The value of 55.5 is the water concentration in solution by mol L^{-1}. The corresponding results obtained are listed in Table 8.

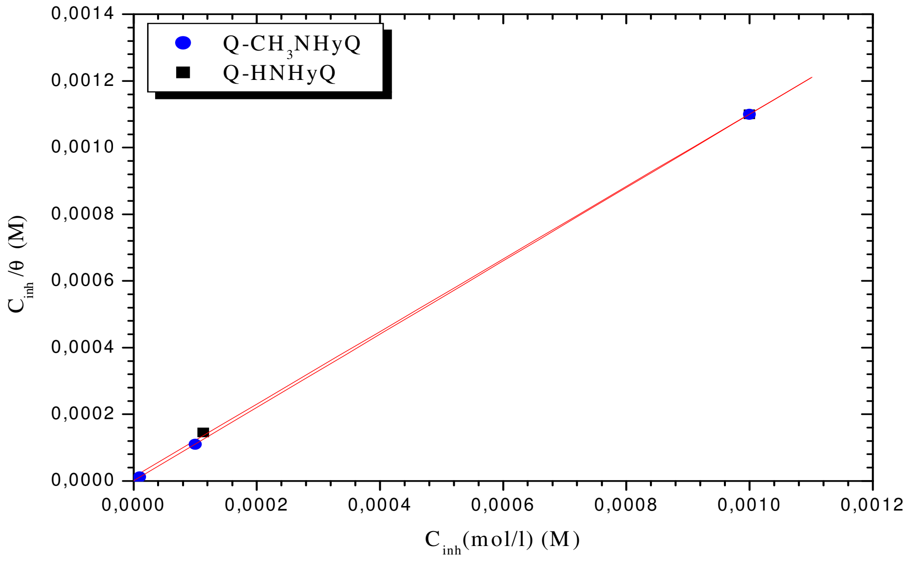

Figure 13: Langmuir adsorption isotherm of the studied inhibitors on mild steel surface at 298 K

Table 8. Constant value (K_{ads}) and the free enthalpy calculated for inhibitors from the Langmuir isotherm

Inhibitor	Slopes	K_{ads} (L mol^{-1})	R^2	$-\Delta G^*_{ads}$ (kJ mol^{-1})
Q-CH$_3$NHyQ	1.04	565719.65	0.99999	-42.77
Q-HNHyQ	1.10	366517.86	0.99998	-41.69

Generally it is observed that if the value of ΔG^*_{ads} is around -40 kJ mol^{-1} or more negative, it suggests chemisorption where charge sharing or charge transfer from an organic species to the metal surface occurs in order to form a coordinate type metallic bond. On the other hand, a value of around -20 kJ mol^{-1} or less negative are coherent with physisorption. The adsorption process is due to electrostatic interactions between the charged molecules and the charged metal surface [59-61]. By inspecting the data in Table 8, the values of ΔG^*_{ads} for **Q-CH$_3$NHyQ** and **Q-HNHyQ** are -42.77 kJmol^{-1} and -41.69 kJmol^{-1}, respectively, which indicate that the adsorption mechanism of these inhibitors on the metal surface in 1 M HCl is typical of chemical adsorption.

3.6. Characterization of the surface area by scanning electron microscopy (SEM)

SEM is based on the principle of electron-matter interactions, capable of producing high resolution images of the surface of a sample. The SEM principle consists of an electron beam scanning the surface of the sample to be analyzed that, in response, re-emits certain particles. These particles are analyzed by different detectors, which make it possible to reconstruct a three-dimensional image of the surface [62-69].

In order to evaluate the morphology of the surface of the steel to prove whether the inhibition is due to the formation of a film of organic molecules on its surface, we have used scanning electron microscopy (SEM). The image of the surface of the mild steel after 24 hours of immersion at 298 K in 1 M HCl alone (Figure14) shows clearly that the surface of the steel has undergone corrosion in the absence of the inhibitors.

On the other hand, in the presence of the inhibitors **Q-CH$_3$NHyQ** and **Q-HNHyQ**, we observe on the images of the mild steel surface after 24 h immersion in 1 M HCl medium at 298 K in the presence of 10^{-3} M of **Q-CH$_3$NHyQ** (Fig.15) and **Q-HNHyQ** (Fig.16). On the basis of these figures, it is obvious, that the surface is covered with a product in the form of a plate indicating the presence of an organic product. This observation shows that the inhibition is due to the formation of an adherent, stable and insoluble deposit, which limits the access of the electrolyte to the surface of the steel.

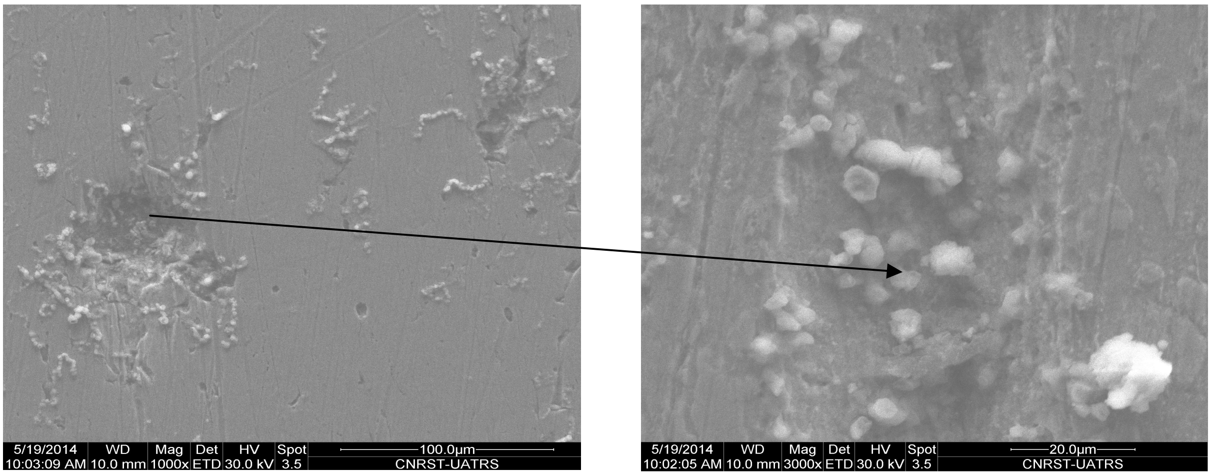

Figure 14: SEM images of mild steel after immersion for 24 h in 1 M HCl

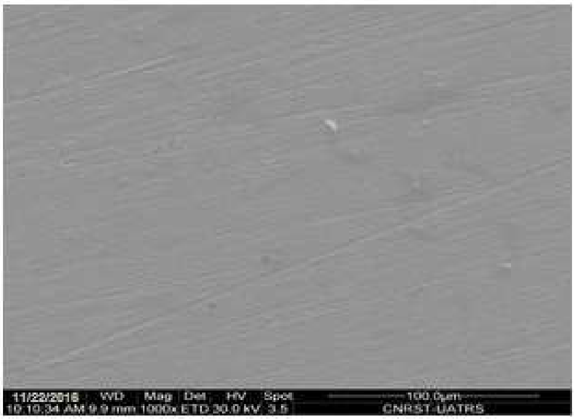

Figure 15: SEM images of mild steel after immersion in 1 M HCl solution in the presence of 10^{-3} M of **Q-CH$_3$NHyQ**

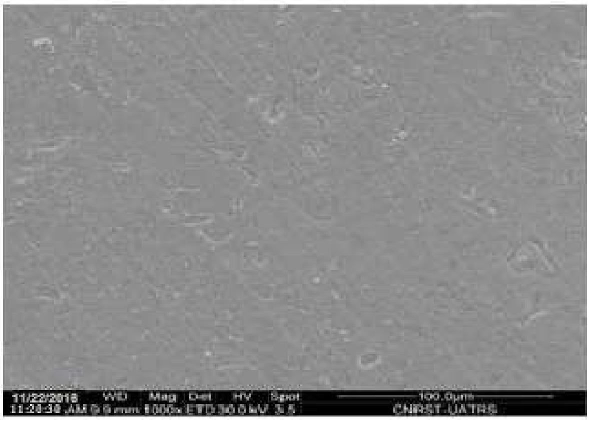

Figure 16: SEM images of mild steel after immersion in 1 M HCl solution in the presence of 10^{-3} M of **Q-HNHyQ**

Conclusion

In the present study, the corrosion inhibition performances of two synthesized 8-hydroxyquinoline derivatives were investigated for mild steel in 1 M HCl medium using different techniques. On the basis of the above results the following conclusions can be drawn:

- These compounds have been synthesized in good yield and act as good corrosion inhibitors of mild steel in 1M HCl medium.
- The inhibition efficiency values obtained by EIS and polarization measurements are in good agreement.
- The studied compounds were found to be mixed-type inhibitors but predominantly anodic.
- EIS measurements showed that charge transfer resistance (R_{ct}) increases and double layer capacitance (C_{dl}) decreases in presence of inhibitors, suggested the adsorption of the inhibitor molecules on the surface of mild steel.
- Adsorption of the studied inhibitors on the mild steel surface obeys the Langmuir adsorption isotherm.
- The SEM analysis showed that the mild steel surface was protected in the presence of both compounds.

Acknowledgements- This work was supported by "*CNRST*"and the "*Moroccan Ministry of Higher Education*".

References

1. M. Galai, M. Rbaa, Y. El Kacimi, M. Ouakki, N. Dkhirech, R. Touir, B. Lakhrissi, M.E. Touhami, *Anal. Bioanal. Electrochem.*, (1) (2017) 80-101.
2. M. Elfaydy, H. Lgaz, R. Salghi, M. Larouj, S. Jodeh, M. Rbaa, B. Lakhrissi, *J. Mater. Environ. Sci.*, 7(9) (2016) 3193-3210.
3. M. Wery, V. Ligier, J. Kirmann, J.C. Catonne, *T. I. Met. Finish.*, 75 (1997) 73-80.
4. L. Larabi, Y. Harek, *Port. Electrochim. Acta.*, (22) (2004) 227-247.
5. Y. Toudic, R. Aumont, *J. Cryst. Growth.*, 10(2) (1971) 170-174.
6. M. Benabdellah, R. Touzani, A. Aouniti, A. Dafali, S. Elkadiri, B. Hammouti, M. Benkaddour, *Phys. Chem. News.*, (37) (2007) 63-69.
7. L. Larabi, Y. Harek, O. Benali, S. Ghalem, *Progress in Organic Coatings.*, 54(3) (2005) 256-262.
8. A. Zarrouk, B. Hammouti, H. Zarrok, R. Salghi, A. Dafali, L. Bazzi, L. Bammou, S.S. Al-Deyab, *Der Pharm. Chem.*, 4(1) (2012) 337-346.
9. H. Zarrok, R. Saddik, H. Oudda, B. Hammouti, A. El Midaoui, A. Zarrouk, N. Benchat, Ebn Touhami M., *Der Pharm. Chem.*, 3(5) 2011) 272-282.
10. A. Zarrouk, B. Hammouti, R. Touzani, S.S. Al-Deyab, M. Zertoubi, A. Dafali, S. Elkadiri , *Int. J. Electrochem. Sci.*, 6 (10) (2011) 4939-4952.
11. M. Rbaa, M. Galai, Y. El Kacimi, M. Ouakki, R. Touir, *Portugaliae Electrochimica Acta.*, 35(6) (2017) 323-338.
12. A. Zarrouk, H. Zarrok, R. Salghi, R. Touir, B. Hammouti, N. Benchat, L.L. Afrine, H. Hannache, M. El Hezzat, M. Bouachrine, *J. Chem. Pharm. Res.*, 5(12) (2013) 1482-1491.
13. H. Zarrok, A. Zarrouk, R. Salghi, M. Ebn Touhami, H. Oudda, B. Hammouti, R. Touir, F. Bentiss F, S.S. Al-Deyab, *Int. J. Electrochem. Sci.*, 8(4) (2013) 6014-6032.
14. D. Ben Hmamou, M.R. Aouad, R. Salghi, A. Zarrouk, M. Assouag, O. Benali, M. Messali, H. Zarrok, B. Hammouti, *J. Chem. Pharm. Res.*, 2012, 4(7), 34984-3504.
15. H.F. Finley, N. Hackerman, *J. Electrochem. Soc.*, 107(4) (1960) 259-263.
16. M. Mahdavian, S. Ashhari, *Electrochim. Acta.*, 55(5) (2010) 1720-1724.
17. X. Wang, H. Yang, F. Wang, *Corros. Sci.*, 53(1) (2011)113-121.
18. A.S. Fouda, M. Abdallah, R.A. El-Dahab, *Desalination and Water Treatment.*, 22(1-3) (2010) 340-348.
19. I. El Ouali, B. Hammouti, A. Aouniti, Y. Ramli, M. Azougagh, E.M. Essassi, M. Bouachrine, J. *Mater. Environ. Sci.*, 1(1) (2010) 1-8.
20. M. Elayyachy, B. Hammouti, A. El Idrissi, A. Aouniti, *Port. Electrochim. Acta.*, 29(1) (2011) 57-68.
21. A. Zarrouk, A. Dafali, B. Hammouti, H. Zarrok, S. Boukhris, M. Zertoubi, *Int. J. Electrochem. Sci.*, 5 (2010) 46-55.
22. Y. Karzazi, M.E. Belghiti, F. El-Hajjaji, B. Hammouti, *J. Mater. Environ. Sci.* 7 (10) (2016) 3916-3929.
23. A. Zarrouk, H. Zarrok, R. Salghi, B. Hammouti, S.S. Al-Deyab, R. Touzani, T.B.A. Hadda, *Int. J. Electrochem. Sci.*, 7 (2012) 6353-6364.
24. J. Fu, H. Zang, Y. Wang, S. Li, T. Chen, X. Liu, *Ind. Eng. Chem. Res.*, 51 (2012) 6377-6386.
25. I.B. Obot, N.O. Obi-Egbedi, *Curr. Appl. Phys.*, 11 (2011) 382-392.
26. K. Adardour, O. Kassou, R. Touir, M.E. Touhami, H. El Kafsaoui, H. Benzeid, M. Sfaira, *J. Mater. Environ. Sci.*, 1 (2010) 129-138.
27. M. Rbaa, M. Galai, M. EL Faydy, Y. El Kacimi, M. Ebn Touhami, A. Zarrouk, B. Lakhrissi, *J. Mater. Environ. Sci.*, 8(10) (2017) 3529-3549.
28. M. El Faydy, M. Galai, R. Touir, A. El Assyry, M. Ebn Touhami, B. Benali, B. Lakhrissi, A. Zarrouk, *J. Mater. Environ. Sci.*, 7(4) (2016) 1406-141.
29. J. Ohmori, S. Sakamoto, H. Kubota, M. Shimizu-Sasamata, M. Okada, S. Kawasaki, *J. Med. Chem.*, 37(4) (1994) 467-475.
30. L. Feng, X. Wang, Z. Chen, *Spectrochim. Acta Part A: Mol. Biomol. Spectr.*, 71(2) (2008) 312-316.
31. Z. Wang, A. Chetouani, B. Hammouti, A. Aouniti, N.P. Benchat, T. Benhadda, *Int. J. Electrochem. Sci.*, 45 (2012) 373-378.
32. L. Larabi, Y. Harek, M. Traisnel, A. Mansri, *J. Appl. Electrochem.*, 34(8) (2004) 833-839.

33. S. Ghareba, S. Omanovic, *Corros. Sci.,* 52 (2010) 2104-2113.
34. H. Gerengi, K. Darowicki, G. Bereket, P. Slepski, *Corros. Sci.*, 51 (2009) 2573-2759.
35. M. Lebrini, M. Lagrenée, H. Vezin, M. Traisnel, F. Bentiss, *Corros. Sci.*, 49(5) (2007) 2254-2269.
36. L. Larabi, O. Benali, Y. Harek, *Port. Electrochim. Acta.*, 24(3) (2006) 337-346.
37. L.R. Chauhan, G. Gunasekaran, *Corros. Sci.*, 49(3) (2007) 1143-1161.
38. J.C. da Rocha, J.A.D.C.P. Gomes, E. D'Elia, *Corros. Sci.*, 52(7) (2010) 2341-2348.
39. M. Bhardwaj, R. Balasubramaniam, *Int. J. Hydrogen. Energ.,* 33(9) (2008) 2178-2188.
40. G. Goldet, C. Brandmayr, S.T. Stripp, T. Happe, C. Cavazza, J.C. Fontecilla-Camps, F.A. Armstrong , *J. Am. Chem. Soc.*, 131(41) (2009) 14979-14989.
41. A. Aouniti, B. Hammouti, M. Brighli, S. Kertit, F. Berhili, S. El-Kadiri, A. Ramdani, A., *J. Chim Phy.*, 93(1996) 1262-1280.
42. H.H. Hassan, *Electrochim. Acta.*, 53(4) (2007) 1722-1730.
43. M.A. Quraishi, H.K. Sharma, *Mater. Chem. Phys.*, 78(1) (2003) 18-21.
44. Z. Tao, S. Zhang, X. Li, B. Hou, *Corros. Sci.*, 51(11) (2009) 2588-2595.
45. F. Bentiss, M. Lagrenee, M. Traisnel, J.C. Hornez, *Corros. Sci.*, 41(4) (1999) 789-803.
46. H.L. Wang, H.B. Fan, J.S. Zheng, *Mater. Chem. Phys.*, 77(3) (2003) 655-661.
47. E.A. Noor, A.H. Al-Moubaraki, *Mater. Chem. Phys.*, 110(1) (2008) 145-154.
48. A. Ghazoui, N. Benchat, F. El-Hajjaji, M. Taleb, Z. Rais, R. Saddik, A. Elaatiaoui, B. Hammouti, *Journal of Alloys and Compounds*, 693 (2017) 510-517.
49. E.E. Ebenso, I.B. Obot, L.C. Murulana, *Int. J. Electrochem. Sci.*, 5 (2010) 1574-1586.
50. H. Zarrok, A. Zarrouk, R. Salghi, M. Assouag, B. Hammouti, H. Oudda, I. Warad, Der Pharmacia Lettre, 5(2013)43-53.
51. M.A. Azaroual, E.F. El Harrak, R. Touir, A. Rochdi, M.E. Touhami, *J. Mol. Liq.*, 220 (2016) 549-557.
52. S. Martinez, I. Stern, *Appl. Surf. Sci.*, 199 (2008) 83-89.
53. P.M. Wadhwani, D.G. Ladha, V.K. Panchal, N.K. Shah, *RSC Advances*, 5(10) (2015)7098-7111.
54. A. El Ouafi, B. Hammouti, H. Oudda, S. Kertit, M. Benkaddour, T. Ben-Hadda, *Ann. Chim. Sci.* Mat., 27 (2002) 71-80.
55. K. Adardour, R. Touir, R.A. Belakhmima, M.E. Touhami, C.K. Mubengaji, E.M. Essassi, *Res. Chem. Intermed.*, 39 (2013) 1843-1855.
56. Y. Abboud, A. Abourriche, T. Saffaj, M. Berrada, M. Charrouf, A. Bennamara, H. Hannache, *Mat. Chem. Phys.*, 105(1) (2007) 1-5.
57. M. Benabdellah, R. Touzani, A. Aouniti, A. Dafali, S. Elkadiri, B. Hammouti, M. Benkaddour, *Phys. Chem. News.*, (37) (2007) 63-69.
58. D.K. Yadav, M.A. Quraishi, *Ind. Eng. Chem. Res.*, 51(46) (2012) 14966-14979.
59. E. Khamis, F. Bellucci, R.M. Latanision, E.S.H. El-Ashry, *Corros.*, 47(9) (1991) 677-686.
60. F.M. Donahue, K. Nobe K, *J. Electrochem. Soc.*, 112(9) (1965) 886-891.
61. L. Larabi, O. Benali, Y. Harek, *Port. Electrochim. Acta.*, 24(3) (2006) 337-346.
62. L.O. Olasunkanmi, I.B. Obot, M. Kabanda, E.E. Ebenso, *J. Phys. Chem.*, 119(28) (2015) 16004-16019.
63. F. Bentiss, M. Traisnel, L. Gengembre, M. Lagrenée, *Appl. Surf. Sci.*, 152(3) (1999) 237-249.
64. W.H. Li, Q. He, S.T. Zhang , C.L. Pei, B.R. Hou , *J. Appl. Electrochem.*, 38(3) (2008) 289-295.
65. W. Li, Q. He, C. Pei, B. Hou, *Electrochim. Acta.,* 52(22) (2007) 6386-6394.
66. F. Xu, J. Duan, S. Zhang, B. Hou, *Mater. Lett.*, 62(25) (2008) 4072-4074.
67. S. Ramesh, S. Rajeswari, S. Maruthamuthu, *Appl. Surf. Sci.*, 229(1) (2004) 214-225.
68. Y. Tang, F. Zhang, S. Hu, Z. Cao, Z. Wu, W. Jing , *Corros. Sci.*, 74 (2013) 271-282.
69. E.S.M. Sherif, A.A. Almajid, *J. Appl. Electrochem.*, 40(8) (2010) 1555-1562.

(2018) ; http://www.jmaterenvironsci.com